ONLINE FIRST

ISSN: 0015-5659

e-ISSN: 1644-3284

Digital image analysis of vertebral body L4 and its ossification center in the human fetus

Authors: Mariusz Baumgart, Magdalena Grzonkowska, Michał Kułakowski

DOI: 10.5603/fm.101420

Article type: Original article

Submitted: 2024-07-02

Accepted: 2024-09-17

Published online: 2024-10-14

Digital image analysis of vertebral body L4 and its ossification center in the human fetus

Mariusz Baumgart[1, *], Magdalena Grzonkowska[1, *], Michał Kułakowski[2]

[1]Department of Normal Anatomy, the Ludwik Rydygier *Collegium Medicum* in Bydgoszcz, the Nicolaus Copernicus University in Toruń, Poland

[2]Clinical Department of Orthopedics and Traumatology, Jan Biziel University Hospital No. 2 in Bydgoszcz, Nicolaus Copernicus University in Toruń, Poland

[*]These authors have equal contributions to this article.

Address for correspondence:
Magdalena Grzonkowska, MD
Department of Normal Anatomy,
the Ludwik Rydygier *Collegium Medicum* in Bydgoszcz,
Łukasiewicza 1 St, 85–821 Bydgoszcz, Poland
tel. + 48 052 5853705
e-mail: m.grzonkowska@cm.umk.pl

ABSTRACT

Using a Siemens-Biograph 128 mCT camera the morphometric analysis of the L4 vertebral body and its ossification center were done in 55 human fetuses aged 17 to 30 weeks. No sex differences were found. The mean height, transverse and sagittal diameters of L4 vertebral body followed the logarithmic functions: $y = –11.797+ 5.208 \times \ln(age) \pm 0.372$, $y = –23.462 + 9.428 \times \ln(age) \pm 0.702$, $y = 2.770 + 13.521 \times \ln(age) \pm 1.722$, respectively. The mean cross-sectional area of L4 vertebral body followed the linear function: $y = –30.683 + 1.976 \times age \pm 2.701$. The mean volume of L4 vertebral body followed the second-degree polynomial function: $y = –93.983+ 0.385 \times (age)^2 \pm 23.707$. The mean transverse and sagittal diameters of the ossification center of L4 vertebral body followed the natural logarithmic function: $y = –27.106 + 10.178 \times \ln(age) \pm 0.769$ and $y = –13.345 + 5.458 \times \ln(age) \pm 0.424$, respectively. The mean cross-sectional area and the volume of the ossification center of L4 vertebral body followed the linear function: $y = –30.683 + 1.976 \times age \pm 2.701$ and $y = –43.214 + 2.760 \times age \pm 4.085$, respectively.

Keywords: vertebra L4, body ossification center, size, growth dynamics, human fetus

INTRODUCTION

The skeleton is one of the earliest and fastest developing structures during organogenesis, thus making it follow-up relatively easy in the fetal period with the methods of ultrasonography, computerized tomography and magnetic resonance imaging [23, 24, 31].

In prenatal diagnostics, it is paramount to appropriately identify and categorize skeletal dysplasias as their diverse symptoms may be misinterpreted, nevertheless studies of skeletodysplasias have been carried out for over 50 years [21, 28].

As early as in the 1960s, children with disproportionate short stature were diagnosed as achondroplasia (short limbs) or Morquio syndrome (short torso) [6]. Subsequently, numerous diseases were distinguished, which allowed experts to categorize them. In the 1970s, their classification was only based on clinical and descriptive characteristics. Once the genetic background and pathogenesis of individual diseases were identified, their categories evolved on the basis of combined genetic, clinical and radiological features [10, 14, 15, 17]. In the latest (2015) nosological classification, the total number of diseases decreased from 456 to 436, while the number of groups increased from 40 to 42, and the number of genes increased from 226 to 364 in comparison with the 2011 classification. The introduced classification provided significant help for basic research and identification of the genes responsible for each disease [7].

In clinical practice, physicians diagnosing patients with small body height must face a comprehensive list of multiple diseases. Therefore, precise assessment of clinical and radiological symptoms is indispensable for a precise diagnosis. During the intrauterine development, early detection of developmental defects is possible in a routine ultrasound examination, while assessment of the lumbar spine using 3D-ultrasound can be performed at week 16 of gestation onwards [23].

To date, a comprehensive three-dimensional growth of the fetal spine has been established in detail using computed tomography and digital image analysis only for the C2, C4, T6 and L3 vertebrae [3, 4, 26, 27]. Therefore, this study has been focused on advanced morphometric analysis of vertebra L4.

In the present study we aimed:

- to perform morphometric analysis of the L4 vertebral body and its ossification center with respect to their linear, superficial and spatial parameters in order to determine their normative age-specific values;
- to examine possible differences between sexes for the analyzed parameters;
- to compute growth curves for the analyzed parameters, expressed by best-matched mathematical models.

MATERIALS AND METHODS

The study material comprised 55 human fetuses of both sexes (27 males and 28 females) aged 17 to 30 weeks of fetal life, originating from spontaneous miscarriages and preterm deliveries. The fetuses were gathered prior to the year 2000 and remain a part of the fetal collection in the Department of Normal Anatomy. The study received approval from the Bioethics Committee of Ludwik Rydygier *Collegium Medicum* in Bydgoszcz (KB 275/2011). The criteria for including the fetuses in the study were based on an assessment of their distinct morphology and statistical records of the pregnancy progression. Since neither internal nor external notable morphological abnormalities were observed during the macroscopic examination, all specimens included were classified as normal. Importantly, the fetuses did not exhibit any developmental anomalies in the musculoskeletal system. The ages of the fetuses were determined using the crown–rump length (CRL) and the known date of the onset of the last maternal menstrual period. Additionally, the fetuses under investigation did not show signs of growth retardation, as the correlation between the gestational age based on the CRL and that calculated from the last menstruation was $R = 0.98$ ($p < 0.001$). Table 1 presents the characteristics of the study group, including the age, number, and sex of the fetuses.

Using a Siemens-Biograph 128 mCT camera, the fetuses were scanned at a step of 0.4 mm, and the data was recorded in DICOM formats and subsequently subjected to morphometric analysis with the use of the Osirix 3.9 software. (Fig. 1).

The gray scale of achieved CT pictures expressed in Hounsfield units ranged from −275 to −134 for a minimum, and from +1165 to +1558 for a maximum. Thus, the window width altered from 1.404 to 1.692, whereas the window level (WL) varied from +463 to +712. The specifics of the imaging protocol were expressed, as follows: mAs — 60, kV — 80, pitch — 0.35, FoV — 180, rot. time — 0.5 sec., while the specifics of CT data were: slice thickness — 0.4 mm, image increment — 0.6 mm, and kernel — B45 f-medium.

Notwithstanding the cartilaginous developmental stage, precise outlines of the L4 ossification center were already explicitly discernible [9, 11], thus allowing to carry out its morphometric analysis in terms of its linear, planar and spatial parameters.

The following 9 parameters of the L4 vertebral body and its ossification center were defined and measured:

1. body height — the maximum distance between the superior and inferior edges of the vertebral body in the sagittal plane (Fig. 2);
2. transverse diameter of vertebral body — the maximum distance between the lateral edges of the vertebral body in the transverse plane (Fig. 2);
3. sagittal diameter of vertebral body — the maximum distance between the anterior and posterior edges of the vertebral body in the sagittal plane (Fig. 2);
4. transverse diameter of body ossification center — the maximum distance between the lateral edges of the ossification center in the transverse plane (Fig. 2);
5. sagittal diameter of body ossification center — the maximum distance between the anterior and posterior edges of the ossification center in the sagittal plane (Fig. 2);
6. cross-sectional area of vertebral body — based on the determined contour of the vertebral body in the transverse plane (Fig. 2);
7. cross-sectional area of body ossification center — based on the determined contour of the ossification center in the transverse plane (Fig. 2);
8. volume of vertebral body and its ossification center, respectively — calculated using advanced diagnostic imaging tools for 3D reconstruction, taking into account position and absorption of radiation by bone tissue (Fig. 1C, D).

Besides, the ossification center–to–vertebral body volume ratio was introduced to determine the relative volumetric growth of the body ossification center with relation to the vertebral body.

The numerical data obtained was statistically analyzed. Distribution of variables was checked using the Shapiro–Wilk (W) test, while homogeneity of variance was checked using Fisher's test. The results were expressed as arithmetic means with standard deviations (SD). To compare the means, Student’s t-test for independent variables and one-way ANOVA were used, followed by Tukey’s post hoc analysis. If no similarity of variance occurred, the non-parametric Kruskal-Wallis test was used. The characterization of developmental dynamics of the analyzed parameters was based on linear and curvilinear regression analysis. The match between the estimated curves and measurement results was evaluated based on the coefficient of determination (R^2).

In a continuous effort to minimize measurement and observer bias, all measurements were performed by one researcher (M.B.) and verified by the other examiner (M.G.). The intra-class correlation coefficients (ICC) were statistically significant ($p < 0.001$) and of excellent reproducibility, as displayed in Table 2.

RESULTS

Means and standard deviations of all the analyzed parameters for height, transverse and sagittal diameters, cross-sectional area and volume of the L4 vertebral body in human fetuses at varying gestational ages have been presented in Table 3.

The statistical analysis revealed no significant sex differences, which allowed us to compute only one growth curve for each analyzed parameter. The growth dynamics of the height, transverse and sagittal diameters of the L4 vertebral body followed natural logarithmic functions.

The mean height of L4 vertebral body at fetal ages of 18–30 weeks ranged from 2.82 to 6.03 ± 0.64 mm, following the natural logarithmic function : $y = –11.797 + 5.208 \times \ln(age) \pm 0.372$ – (Fig. 3A).

The mean transverse diameter of L4 vertebral body at fetal ages of 18–30 weeks grew from 3.11 to 8.27 ± 0.53 mm, in accordance with the natural logarithmic function: $y = –23.462 + 9.428 \times \ln(age) \pm 0.702$ – (Fig. 3B).

Between weeks 18 and 30, the mean sagittal diameter of L4 vertebral body ranged from 2.91 mm to 6.14 ± 0.13 mm, following the natural logarithmic function: $y = 2.770 + 13.521 \times \ln(age) \pm 1.722$. – (Fig. 3C).

In fetuses aged 17–30 weeks, the mean cross-sectional area of L4 vertebral body ranged from 8.04 to 42.00 ± 1.52 mm^2, in accordance with the linear function: $y = –39.101 + 2.733 \times age \pm 3.868$ – (Fig. 3D).

The mean volume of L4 vertebral body at fetal ages of 18–30 weeks ranged from 22.67 to 253.57 ± 31.36 mm^3, in accordance with the second-degree polynomial function: $y = –93.983 + 0.385 \times (age)^2 \pm 23.707$ — (Fig. 3E).

Means and standard deviations of all the analyzed parameters for transverse and sagittal diameters, cross-sectional area, and volume of the ossification center of the L4 vertebral body in human fetuses at varying gestational ages have been presented in Table 4.

The mean transverse diameter of the ossification center of L4 vertebral body at fetal ages of 18–30 weeks ranged from 1.29 to 7.15 ± 0.64 mm, in accordance with the natural logarithmic function: y = –27.106 + 10.178 × ln(age) ± 0.769 – (Fig. 4A).

The mean sagittal diameter of the ossification center of L4 vertebral body at fetal ages of 18–30 weeks ranged from 1.95 to 5.51 ± 0.33 mm, in accordance with the natural logarithmic function: y = –13.345 + 5.458 × ln(age) ± 0.424 — (Fig. 4B).

The mean cross-sectional area of the ossification center of L4 vertebral body at fetal ages of 18–30 weeks ranged from 4.85 to 27.18 ± 2.26 mm^2, in accordance with the linear function: y = –30.683 + 1.976 × age ± 2.701 — (Fig. 4C).

In fetuses aged 17–30 weeks, the mean volume of the ossification center of L4 vertebral body ranged from 4.60 to 40.45 ± 3.25 mm^3, in accordance with the linear function: y = –43.214 + 2.760 × age ± 4.085 — (Fig. 4D).

In the study period, the mean value of the ossification center–to–vertebral body volume ratio for vertebra L4 decreased from 0.21 to 0.16 (Fig. 4E).

DISCUSSION

The process of ossification of vertebrae begins at the embryonic stage and ends at approximately 25 years of age. Initially, the central part of the vertebral body is occupied by two primary ossification centers — ventral and dorsal — that subsequently fuse into one body ossification center [31]. At the beginning of month 3 of gestation, all presacral vertebrae have three ossification centers: one in the body and one in either neural process [11, 18, 23]. Histologically, it is possible to visualize ossification centers in neural processes as early as at the end of week 8 of the embryonic period [31]. According to Bagnall et al. [1], first ossification centers in the body and neural processes of lumbar vertebrae can already be noticeable in fetuses with crown-rump length (CRL) of 51 mm. In turn, Bareggi et al. [2] observed first ossification centers in neural processes of the L1–L4 vertebrae as early as in fetuses with a CRL of 45 mm.

At birth, each vertebra consists of three bony parts interconnected by cartilage. The bony parts of neural processes fuse between 3 and 5 years of age. The ossification process firstly occurs in neural processes of lumbar vertebrae and follows cephalad [31]. The first body ossification centers appear in lower thoracic and upper lumbar vertebrae as early as at approximately week 10 of gestation. Of note, this process simultaneously progresses both cephalad and caudad [18, 31]. Contrariwise, the first ossification centers of neural processes can be initially observed in upper cervical vertebrae, starting from the axis, at approximately

week 8 of prenatal life [11]. Of note, such a process progresses caudad [18, 31]. However, this matter is under discussion because some researchers simultaneously found the first ossification centers of neural processes in two sections: cervical, as well as lower thoracic and upper lumbar, concluding that possibly this process starts at two different places [31].

In our material under examination no sex differences concerning all numerical data of vertebra L4 and its body ossification center have been found. This closely corresponds to findings by Mărginean et al. [18], who did not notice any sex differences in the structure of the lumbar vertebrae in human fetuses and neonates.

Widjaja et al. [31] performed measurements of vertebra L2 in human fetuses, concentrating on the height of vertebral body and its surface area, the height of intervertebral disc and the surface area of body ossification center. This authors demonstrated a commensurate increase in the height and surface areas of both vertebral body L2 and its ossification center that followed the linear functions: $y = –0.33 + 0.21 \times age$, $y = –64.62 + 4.82 \times age$, andy $= –43.02 + 2.58 \times age$, respectively. The authors found the thoracic and lumbar vertebrae to grow in height and surface area in a manner proportionate to age, while our present study demonstrated a logarithmic increase in the height of vertebral body L4. The authors also noted that the growth of the intervertebral disc was greater than that of the vertebral body, and pointed out that this should not have been erroneously interpreted as a pathological process that occurred in such diseases as mucopolysaccharidoses and osteogenesis imperfecta, in which a vertebral body was significantly reduced in size compared to an intervertebral disc. Furthermore, in ultrasound examination, these authors observed ossification centers in neural processes of cervical vertebrae in all fetuses aged 18–19 weeks. The first ossification centers of neural processes of thoracic and lumbar segments were also observed at 18–19 weeks of fetal life.

Kędzia et al. [13] carried out autopsy studies in 30 human fetuses aged 8 to 20 weeks, in which neural arches in the lumbar segment were measured. They found vertebra L2 to be largest, and so suggested that it could be a characteristic feature occurring by some stage of the spine development. The L2 and L3 vertebrae may develop faster between weeks 7 and 8 of embryonic life due to the larger size of the spinal cord at the L2/L3 level. The transverse diameter and surface area of the neural processes reached the highest values for the L1 vertebra and gradually decreased caudad, with the L5 vertebra having the smallest neural arch. The ratio of the surface area of the neural ossification center increased rapidly when the fetus reached a CRL of 40 mm. For the L1 vertebra, this value increased until a CRL of 130 mm, for the L2, L3, L4 vertebrae — 160 mm, and for the L5 vertebra — 170 mm.

An increase in the ratio of the ossification center surface area did not correlate with an increase in the surface area of vertebral arches. The neural ossification center was the largest in vertebra L1.

Literature reports describing human fetuses (n = 55) aged 17 to 30 weeks presented a simplified morphometric analysis of 3 ossification centers of all cervical, thoracic and lumbar vertebrae [26], as well as a comprehensive morphometric analysis including growth curves for vertebrae: C2 [3], C4 [4], T6 [26] and L3 [27]. In the present study, the body height, as well as the transverse and sagittal diameters of both vertebral body L4 and its ossification center followed natural logarithmic functions. The body height and transverse diameter, as well the transverse diameter of body ossification center increased following the functions: $y = –11.797+ 5.208 \times \ln(age) \pm 0.372$, $y = –23.462 + 9.428 \times \ln(age) \pm 0.702$, and $y = –27.106 + 10.178 \times \ln(age) \pm 0.769$, respectively. The sagittal diameter of the L4 vertebral body and its ossification center followed the functions: $y = 2.770 + 13.521 \times \ln(age) \pm 1.722$ and $y = –13.345 + 5.458 \times \ln(age) \pm 0.424$, respectively. According to the professional literature, logarithmic growth of the ossification centers was also observed for the transverse and sagittal diameters of the axial dens ($y = –10.752 + 4.276 \times \ln(age) \pm 0.335$ and $y = –4.329 + 2.010 \times \ln(age) \pm 0.182$, respectively) and the axial body ($y = –10.578 + 4.265 \times \ln(age) \pm 0.338$ and $y = –3.934 + 1.930 \times \ln(age) \pm 0.182$, respectively), vertebra C4 ($y = –8.836 + 3.708 \times \ln(age) \pm 0.334$ and $y = –7.748 + 3.240 \times \ln(age) \pm 0.237$, (respectively), vertebra T6 ($y = –14.784 + 6.115 \times \ln(age) \pm 0.458$ and $y = –12.065 + 5.019 \times \ln(age) \pm 0.315$, respectively) and vertebra L3 ($y = –27.610 + 10.341 \times \ln(age) \pm 0.75$ and $y= –13.858 + 5.636 \times \ln(age) \pm 0.41$, respectively).

The present study also demonstrated a directly proportionate increase in the cross-sectional area of the L4 vertebral body and its ossification center, that followed the functions: $y = –39.101 + 2.733 \times age \pm 3.868$ and $y = –30.683 + 1.976 \times age \pm 2.701$, respectively. Of note, a commensurate increase in the cross-sectional area of the ossification center was also demonstrated for the axial dens: $y = –7.102 + 0.520 \times age \pm 0.724$ [3] and axial body: $y = –7.002 + 0.521 \times age \pm 0.726$ [3], vertebra C4: $y = –4.690 + 0.437 \times age \pm 1.172$ [4], vertebra T6: $y = –15.591 + 1.200 \times age \pm 1.470$ [26], and vertebra L3: $y = –32.423 + 2.071 \times age \pm 2.443$ [27].

In this study, we demonstrated that the volume of the L4 vertebral body in relation to fetal age followed the second-degree polynomial function: $y = –93.983+ 0.385 \times (age)^2 \pm 23.707$, and that of the L4 vertebral body ossification centers followed the linear function: $y = –43.214 + 2.760 \times age \pm 4.085$. In turn, the volume of the ossification centers of both the axial

dens and body [3] followed the logarithmic functions: y =– 37.021 + 14.014 × ln(age) ± 1.091 and y = –37.425 + 14.197 × ln(age) ± 1.109, respectively. For the C4 [4], T6 [23] and L3 [27] vertebrae, volumes of vertebral body ossification centers increased in a proportionate manner: y = –5.917 + 0.582 × age ± 1.157 for vertebra C4, y = –22.120 + 1.663 × age ± 1.869 for vertebra T6, and y = –44.200 + 2.823 × age ± 3.76 for vertebra L3.

It is noteworthy that throughout the study period, the ossification center–to–vertebral body volume ratio of vertebra L4 decreased from 0.21 to 0.16. Comparable changes were observed in these ratios for the axial dens, which decreased from 0.22 to 0.19 [3], and for the bodies of the following vertebrae: C2 which decreased from 0.21 to 0.20 [3], C4 which decreased from 0.23 ± 0.04 to 0.21 ± 0.03 [4], T6 which decreased from 0.28 ± 0.07 to 0.21 ± 0.05 [26], and L3 which decreased from 0.24 ± 0.06 to 0.14 ± 0.05 [27].

In human fetuses Szpinda et al. [27] observed that the transverse diameter of body ossification centers in lumbar vertebrae was largest for vertebra L1 (4.94 ± 1.60 mm) and decreased caudad, as follows: 4.89 ± 1.63 mm for vertebra L2, 4.82 ± 1.71 mm for vertebra L3, 4.59 ± 1.62 mm for vertebra L4, and 4.19 ± 1.45 mm for vertebra L5. The sagittal diameter of body ossification center was the largest for vertebra L3 (1.71 ± 0.96 mm), the smallest for vertebra L5 (1.45 ± 1.03 mm), while for the other lumbar vertebrae these values were similar: 1.60 ± 0.61 mm for vertebra L1, 1.63 ± 0.83 mm for vertebra L2, and 1.62 ± 1.07 mm for vertebra L4. The surface area values for body ossification centers were 14.69 ± 6.38 mm^2 for vertebra L1, 15.98 ± 7.95 mm^2 for vertebra L2, 15.48 ± 7.96 mm^2 for vertebra L3, 13.80 ± 7.82 mm^2 for vertebra L4, and 11.98 ± 7.11 mm^2 for vertebra L5. The volume values for body ossification centers remained: 20.77 ± 8.88 mm^3 for vertebra L1, 21.29 ± 12.67 mm^3 for vertebra L2, 21.50 ± 10.95 mm^3 for vertebra L3, 19.78 ± 13.11 mm^3 for vertebra L4, and 16.93 ± 11.04 mm^3 for vertebra L5.

As stated by Kędzia et al. [13], the mean height of lumbar vertebrae measured from their superior to inferior articular processes was 4.71 ± 1.61 mm for vertebra L1, 5.02 ± 1.76 mm for vertebra L2, 4.82 ± 1.77 mm for vertebra L3, 4.39 ± 1.58 mm for vertebra L4, and 3.97 ± 1.44 mm for vertebra L5.

Using ultrasound, Schild et al. [23] measured volumes of lumbar vertebral bodies and the length of the lumbar segment in 289 fetuses aged 16 to 37 weeks. The vertebral volumes followed the functions: y = exp (2.99 – 89.76/age) for vertebra L1, y = exp (2.785 – 86.94/age) for vertebra L5, and y = exp (4.943 – 89.81/age) for vertebrae L1–L5. Furthermore, the length of the lumbar segment followed the function: y = exp (4.705 – 32.4/age). The volume of vertebra L1 for the 50th percentile was 101 mm^3 at week 17, and

998 mm^3 at week 30, while that of vertebra L5 was 53 mm^3 at week 17, and 749 mm^3 at week 30 of gestation. These results supported a decrease in the size of lumbar vertebrae in the caudal direction as well. In the present study with the use of objective and precise morphometric methods, the volume of the L3 vertebra between 17 and 30 weeks of gestation ranged from 22.67 to 253.57 ± 31.36 mm^3.

Pathologies of the lumbar spine are considered lifestyle diseases, however some may refer to changes grounded in the fetal life [13]. The correct development of lumbar vertebrae is critical from a clinical perspective, e. g. a relatively small vertebral canal may cause back pain in adults [27]. The commonest developmental defects of vertebrae are displayed by hemivertebrae, butterfly vertebrae and coronal cleft vertebrae [30]. The onset of a hemivertebra or butterfly vertebra can occur as early as at week 5 during somitogenesis [24]. Since vertebral defects are combined with e.g., kyphosis, scoliosis, or spina bifida, therefore early diagnostics and detection of these anomalies are extremely important.

Spina bifida is a consequence of incomplete closure of bilateral neural processes and occurs in 1 per 1000 births. Some causes of this condition are environmental factors, e.g., insufficient intake of folic acid, or genetic factors. Its mildest form, i.e. spina bifida occulta, is usually asymptomatic if parts of the nervous system are not involved. A tuft of hair over the skin covering the underdeveloped vertebra can be the only sign of this spine pathology. Open spina bifida is a more serious condition, in which a meningeal sac extends through the incomplete neural arch causing neurological deficits of various degrees. Thus, the fetal spinal cord is exposed to mechanical and chemical damage, the latter of which is mainly caused by the amniotic fluid, toxic for developing nerve cells [5, 16, 20]. Until week 15 of gestation, the bilateral neural processes of any vertebra are separated from each other, which is termed physiological spina bifida. The distance between the right and left neural processes at the lumbosacral level is greater than that at the thoracic level. The bilateral neural processes in the thoracic segment fuse at 16–17 weeks of gestation, while those of the lumbosacral segment nearly completely fuse at week 23 of gestation [22]. Early prenatal diagnostics enables the identification of abnormalities in neural process ossification centers and the intervention using intrauterine surgical techniques to minimize the effects of developing pathology [8, 16]. Another congenital defect of the spine is exemplified by congenital scoliosis, *i.e.* lateral deformation of the spine caused by developmental defects of vertebrae that cause imbalance in the longitudinal growth of the spine [22].

Dysplasias of the skeletal system present a large and heterogeneous group of genetic defects characterized by abnormal growth, development, differentiation, and consequently

structure of bone and cartilage. Although their particular incidences are low, their overall incidence is 1 case in 5,000 live births, which constitutes as many as 5% of children born with congenital defects [21]. Because of diagnostic difficulties, the actual incidence of these defects may be much higher [28]. Osteochondrodysplasia is typically manifested by small body height in childhood. The spectrum of symptoms ranges from early arthritis in people with an average body height to severe growth disorders resulting in prenatal death. Such a disorder can affect both the limbs and spine. Furthermore, potential disturbances of the respiratory, circulatory, excretory and nervous systems can occur, along with dysfunction of the sense organs (vision, audition) and psychological problems [6, 10, 14, 15, 17, 19, 20]. Sometimes it is unknown what the direct cause of small body height is: a disease of bone or a systemic disorder. As a prerequisite, endocrine, cardiac, pulmonary and renal disorders should always be ruled out. Differential diagnosis must take into account the proportionality of the body. In children with skeletal dysplasias, disproportions are usually explicitly visible. It should also be considered that some genetic syndromes involve intrauterine growth arrest, however, they should be easily distinguishable using other phenotypic features, dysmorphic characteristics of the face, developmental delay or, if necessary, radiography [10, 17, 19, 31].

Most skeletal dysplasias have their own distinctive radiological features observed in growing bones and cartilages. A complete radiographic examination covering the spine, as well as the epiphyses, metaphyses and diaphyses of bones, should be performed. In epiphyseal dysplasia, absent or small or irregular ossification points of bone epiphyses can be observed. Metaphyseal dysplasia is characterized by irregular, enlarged metaphyses. In turn, diaphyseal dysplasia affecting shafts of long bones causes their enlargement, sclerotization, thickening of the cortical layer, a thinning or enlargement of the medullary cavity. Some pathological changes in long bones may also be accompanied by pathological changes in the spine, e.g. spondylodysplasia. It is also indispensable to assess mineralization and bone age. Diseases involving reduced mineralization of bone are known as osteogenesis imperfecta and hypophosphatasia. In Laron’s syndrome (receptor insensitivity to growth hormone), bone age is considerably delayed [6, 12, 14, 15, 20].

CONCLUSIONS

1. No sex differences are observed in the numerical data of vertebral body L4 and its ossification center.

2. The L4 vertebral body grows logarithmically in its height, transverse and sagittal diameters, linearly in its cross-sectional area, and second-order polynomially in its volume.
3. The body ossification center of vertebra L4 grows logarithmically in its transverse and sagittal diameters, and linearly in its cross-sectional area and volume.
4. The size and growth dynamics of vertebral body L4 and its ossification center are relevant in anomalies of the spine and skeletal dysplasias.

ARTICLE INFORMATION AND DECLARATIONS

Data availability statement

Any additional data supporting this study are available from the corresponding author (M.G.) upon reasonable request.

Ethics statement

This material has not been published in whole or in part elsewhere.

The manuscript is not currently being considered for publication in another journal. The anatomical protocol of the study was accepted by the Bioethics Committee of Ludwik Rydygier Collegium Medicum in Bydgoszcz (KB 275/2011). The fetuses were obtained from spontaneous abortions after parental consent and were from Department of Anatomy of Ludwik Rydygier *Collegium Medicum* of Nicolaus Copernicus. Everything was in accordance with the legal procedures in force in Poland and in accordance with the program Donation Corpse both adults and fetuses. This study was performed in line with the principles of the Declaration of Helsinki.

Author contributions:

Protocol/project development: Baumgart, Grzonkowska.

Data collection and management: Baumgart, Grzonkowska.

Data analysis: Baumgart, Grzonkowska.

Manuscript writing/editing: Baumgart, Grzonkowska, Kułakowski.

Funding

This research did not receive any specific grant from funding agencies in the public, commercial, or not-for-profit sectors.

Acknowledgments

The authors sincerely thank those who donated their bodies to science so that anatomical research could be performed. Results from such research can potentially increase mankind's overall knowledge that can then improve patient care. Therefore, these donors and their families deserve our highest gratitude.

Conflict of interest

The authors declare that they have no conflict of interest.

REFERENCES

1. Bagnall KM, Harris PF, Jones PR. A radiographic study of the human fetal spine. 2. The sequence of development of ossification centres in the vertebral column. J Anat. 1977; 124(Pt 3): 791–802, indexed in Pubmed: 604345.
2. Bareggi R, Grill V, Zweyer M, et al. A quantitative study on the spatial and temporal ossification patterns of vertebral centra and neural arches and their relationship to the fetal age. Ann Anat. 1994; 176(4): 311–317, doi: 10.1016/s0940-9602(11)80502-9, indexed in Pubmed: 8085652.
3. Baumgart M, Wiśniewski M, Grzonkowska M, et al. Digital image analysis of ossification centers in the axial dens and body in the human fetus. Surg Radiol Anat. 2016; 38(10): 1195–1203, doi: 10.1007/s00276-016-1679-9, indexed in Pubmed: 27130209.
4. Baumgart M, Szpinda M, Szpinda A. New anatomical data on the growing C4 vertebra and its three ossification centers in human fetuses. Surg Radiol Anat. 2013; 35(3): 191–203, doi: 10.1007/s00276-012-1022-z, indexed in Pubmed: 22986651.
5. Beuls EAM, Vanormelingen L, van Aalst J, et al. In vitro high-field magnetic resonance imaging-documented anatomy of a fetal myelomeningocele at 20 weeks' gestation. A contribution to the rationale of intrauterine surgical repair of spina bifida. J Neurosurg. 2003; 98(2 Suppl): 210–214, doi: 10.3171/spi.2003.98.2.0210, indexed in Pubmed: 12650407.
6. Bober MB, Taylor M, Heinle R, et al. Achondroplasia-hypochondroplasia complex and abnormal pulmonary anatomy. Am J Med Genet A. 2012; 158A(9): 2336–2341, doi: 10.1002/ajmg.a.35530, indexed in Pubmed: 22888019.
7. Bonafe L, Cormier-Daire V, Hall C, et al. Nosology and classification of genetic skeletal disorders: 2015 revision. Am J Med Genet A. 2015; 167A(12): 2869–2892, doi: 10.1002/ajmg.a.37365, indexed in Pubmed: 26394607.

8. Bruner JP, Tulipan N, Paschall RL, et al. Fetal surgery for myelomeningocele and the incidence of shunt-dependent hydrocephalus. JAMA. 1999; 282(19): 1819–1825, doi: 10.1001/jama.282.19.1819, indexed in Pubmed: 10573272.
9. Chano T, Matsumoto K, Ishizawa M, et al. Analysis of the presence of osteocalcin, S-100 protein, and proliferating cell nuclear antigen in cells of various types of osteosarcomas. Eur J Histochem. 1996; 40(3): 189–198, indexed in Pubmed: 8922947.
10. Digilio MC, Marino B, Giannotti A, et al. Atrioventricular canal defect and postaxial polydactyly indicating phenotypic overlap of Ellis-van Creveld and Kaufman-McKusick syndromes. Pediatr Cardiol. 1997; 18(1): 74–75, doi: 10.1007/s002469900116, indexed in Pubmed: 8960501.
11. Duarte WR, Shibata T, Takenaga K, et al. S100A4: a novel negative regulator of mineralization and osteoblast differentiation. J Bone Miner Res. 2003; 18(3): 493–501, doi: 10.1359/jbmr.2003.18.3.493, indexed in Pubmed: 12619934.
12. Hassanzadeh M, Rastegar K, Hedayatizadeh M, et al. Evaluation of split cord malformation between years 2006 and 2020: A case series study. Transl Res Anat. 2023; 32: 100251, doi: 10.1016/j.tria.2023.100251.
13. Kedzia A, Czyz M. Ossification process and lumbar spine morphology in the prenatal period. Med Sci Monit. 2003; 9(9): BR343–BR350, indexed in Pubmed: 12960924.
14. Khan S, Hinks J, Shorto J, et al. Some cases of common variable immunodeficiency may be due to a mutation in the SBDS gene of Shwachman-Diamond syndrome. Clin Exp Immunol. 2008; 151(3): 448–454, doi: 10.1111/j.1365-2249.2007.03556.x, indexed in Pubmed: 18190602.
15. Kiel EA, Frias JL, Victorica BE. Cardiovascular manifestations in the Larsen syndrome. Pediatrics. 1983; 71(6): 942–946, indexed in Pubmed: 6856406.
16. Lee W, Chaiworapongsa T, Romero R, et al. A diagnostic approach for the evaluation of spina bifida by three-dimensional ultrasonography. J Ultrasound Med. 2002; 21(6): 619–626, doi: 10.7863/jum.2002.21.6.619, indexed in Pubmed: 12054297.
17. Vakkilainen S, Taskinen M, Klemetti P, et al. Increased mortality in cartilage — hair hypoplasia. Arch Dis Child. 2001; 84(1): 65–67, doi: 10.1136/adc.84.1.65, indexed in Pubmed: 11124791.
18. Mărginean OM, Mîndrilă I, Damian CM, et al. Contributions on the morphometric study of the newborn and fetus spine. Romanian Journal of Functional & Clinical, Macro- & Microscopica. 2011; 10(4): 423.
19. Naidoo N, Khan R, Abdulwahab T, et al. A novel reconstructive approach of the lumbar vertebral column from 2D MRI to 3D models. Transl Res Anat. 2022; 29: 100229, doi: 10.1016/j.tria.2022.100229.
20. Nalla S, Sanchis-Gimeno J, Paton G. Prevalence of sacral spina bifida occulta with lumbosacral transitional vertebra in a skeletal collection of a South African population. Transl Res Anat. 2024; 36: 100307, doi: 10.1016/j.tria.2024.100307.
21. Orioli IM, Castilla EE, Barbosa-Neto JG. The birth prevalence rates for the skeletal dysplasias. J Med Genet. 1986; 23(4): 328–332, doi: 10.1136/jmg.23.4.328, indexed in Pubmed: 3746832.

22. Pooh R. Neuroscan of Normal and Abnormal Vertebrae and Spinal Cord. Donald Sch J Ultrasound Obstet Gynecol. 2009; 2(3): 9–18, doi: 10.5005/jp-journals-10009-1062.

23. Schild RL, Wallny T, Fimmers R, et al. The size of the fetal thoracolumbar spine: a three-dimensional ultrasound study. Ultrasound Obstet Gynecol. 2000; 16(5): 468–472, doi: 10.1046/j.1469-0705.2000.00256.x, indexed in Pubmed: 11169332.

24. Skórzewska A, Grzymisławska M, Bruska M, et al. Ossification of the vertebral column in human foetuses: histological and computed tomography studies. Folia Morphol. 2013; 72(3): 230–238, doi: 10.5603/fm.2013.0038, indexed in Pubmed: 24068685.

25. Szpinda M, Baumgart M, Szpinda A, et al. Cross-sectional study of the ossification center of the C1-S5 vertebral bodies. Surg Radiol Anat. 2013; 35(5): 395–402, doi: 10.1007/s00276-012-1045-5, indexed in Pubmed: 23192240.

26. Szpinda M, Baumgart M, Szpinda A, et al. Morphometric study of the T6 vertebra and its three ossification centers in the human fetus. Surg Radiol Anat. 2013; 35(10): 901–916, doi: 10.1007/s00276-013-1107-3, indexed in Pubmed: 23543237.

27. Szpinda M, Baumgart M, Szpinda A, et al. New patterns of the growing L3 vertebra and its 3 ossification centers in human fetuses – a CT, digital, and statistical study. Med Sci Monit Basic Res. 2013; 19: 169–180, doi: 10.12659/msmbr.883956.

28. Unger S. A genetic approach to the diagnosis of skeletal dysplasia. Clin Orthop Relat Res. 2002(401): 32–38, doi: 10.1097/00003086-200208000-00006, indexed in Pubmed: 12151880.

29. Wallny T, Schild RL, Fimmers R, et al. Three-dimensional sonographic evaluation of the fetal lumbar spinal canal. J Anat. 2002; 200(5): 439–443, doi: 10.1046/j.1469-7580.2002.00048.x, indexed in Pubmed: 12090390.

30. Wei Q, Cai A, Wang X, et al. Value of 3-dimensional sonography for prenatal diagnosis of vertebral formation failure. J Ultrasound Med. 2013; 32(4): 595–607, doi: 10.7863/jum.2013.32.4.595, indexed in Pubmed: 23525384.

31. Widjaja E, Whitby EH, Paley MNJ, et al. Normal fetal lumbar spine on postmortem MR imaging. AJNR Am J Neuroradiol. 2006; 27(3): 553–559, indexed in Pubmed: 16551992.

32. Żytkowski A, Tubbs R, Iwanaga J, et al. Anatomical normality and variability: Historical perspective and methodological considerations. Transl Res Anat. 2021; 23: 100105, doi: 10.1016/j.tria.2020.100105.

Table 1 Age, number and sex of the fetuses studied.

Gestational age	**Crown-rump length [mm]**				**Number of fetuses**	**Sex**	
Weeks (Hbd-life)	Mean	SD	Min.	Max.		♂	♀
17	115.00		115.00	115.00	1	0	1
18	133.33	5.77	130.00	140.00	3	1	2

19	149.50	3.82	143.00	154.00	8	3	5
20	161.00	2.71	159.00	165.00	4	2	2
21	174.75	2.87	171.00	178.00	4	3	1
22	185.00	1.41	183.00	186.00	4	1	3
23	197.60	2.61	195.00	202.00	5	2	3
24	208.67	3.81	204.00	213.00	9	5	4
25	214.00		214.00	214.00	1	0	1
26	229.00	5.66	225.00	233.00	2	1	1
27	237.50	3.33	233.00	241.00	6	6	0
28	249.50	0.71	249.00	250.00	2	0	2
29	253.00	0.00	253.00	253.00	2	0	2
30	263.25	1.26	262.00	265.00	4	3	1
Total					55	27	28

SD — standard deviation.

Table 2. Intra-class correlation coefficients (ICC) values for inter-observer recurrence.

Parameter of the body of veterbra L4	ICC
Height	0.995*
Transverse diameter	0.996*
Sagittal diameter	0.994*
Cross-sectional area	0.996*
Volume	0.997*
Parameter of the body ossification center of veterbra L4	
Transverse diameter	0.996*
Sagittal diameter	0.995*
Cross-sectional area	0.998*
Volume	0.996*

Intra-class correlation coefficients marked with * are statistically significant at $p < 0.0001$.

Table 3. Height, transverse and sagittal diameters, cross-sectional area and volume of the body of vertebr L4.

Gestational age (weeks)	N	Body of veterbra L4				
		Height [mm]	Transverse diameter [mm]	Sagittal diameter	Cross-sectional area [mm^2]	Volume [mm^3]

		[mm]									
		Mean	SD	Mean	SD	Mean	SD	Mean	SD	Mean	SD
17	1	2.82		3.11		2.91		8.04		22.67	
18	3	3.49	0.30	3.89	0.56	2.77	0.25	13.17	3.01	46.45	13.67
19	8	3.35	0.24	3.72	0.34	3.60	0.56	10.18	0.63	34.09	3.06
20	4	3.53	0.42	4.53	0.40	4.11	0.45	12.73	2.43	45.49	13.82
21	4	4.40	0.41	5.93	0.54	3.68	0.06	17.45	0.85	77.03	10.07
22	4	4.30	0.35	6.04	0.66	4.25	0.28	24.80	0.96	106.77	12.04
23	5	4.47	0.41	6.30	0.43	4.54	0.28	22.86	2.22	102.05	12.75
24	9	4.79	0.23	6.61	0.88	5.14	0.40	26.10	3.08	124.80	13.99
25	1	4.83		6.53		5.17		23.20		112.06	
26	2	4.91	0.11	7.49	0.04	5.64	0.89	38.07	0.75	186.69	0.36
27	6	5.10	0.41	7.07	1.03	4.98	0.43	33.67	4.73	172.96	35.70
28	2	6.01	0.13	9.10	0.75	5.99	0.70	42.40	2.83	254.64	11.60
29	2	5.21	0.02	6.70	0.01	6.50	0.01	30.45	0.07	158.49	1.01
30	4	6.03	0.64	8.27	0.53	6.14	0.13	42.00	1.52	253.57	31.33

SD — standard deviation.

Table 4. Transverse diameter, sagittal diameter, cross-sectional area and volume of the ossification center of the body ossification of vertebra L4.

Gestational age (weeks)	**N**	**Body ossification center of veterbra L4**							
		Transverse diameter [mm]		**Sagittal diameter [mm]**		**Cross-sectional area [mm^2]**		**Volume [mm^3]**	
		Mean	SD	Mean	SD	Mean	SD	Mean	SD
17	1	1.29		1.95		4.85		4.60	
18	3	1.93	0.25	2.48	0.19	7.67	1.18	6.26	2.06
19	8	2.13	0.53	2.42	0.35	4.33	0.77	9.73	1.04
20	4	3.24	0.13	3.22	0.32	7.97	2.11	11.65	2.47
21	4	4.87	0.51	3.37	0.08	12.28	1.16	16.30	1.94
22	4	5.11	0.89	3.51	0.44	12.90	1.12	17.00	1.35
23	5	4.94	0.35	3.64	0.45	13.64	1.79	18.2	2.61

24	9	5.22	0.86	4.13	0.41	15.58	2.19	6 21.20	3.84
25	1	5.33		3.85		15.88		22.20	
26	2	6.03	0.45	4.78	0.44	22.95	0.21	36.85	3.75
27	6	6.04	1.11	4.37	0.47	23.25	2.58	29.40	3.72
28	2	6.54	0.81	4.55	0.90	28.25	2.90	36.70	5.09
29	2	6.80	0.02	4.98	0.05	23.25	0.07	31.45	0.07
30	4	7.15	0.64	5.51	0.33	27.18	2.26	40.45	3.25

SD — standard deviation.

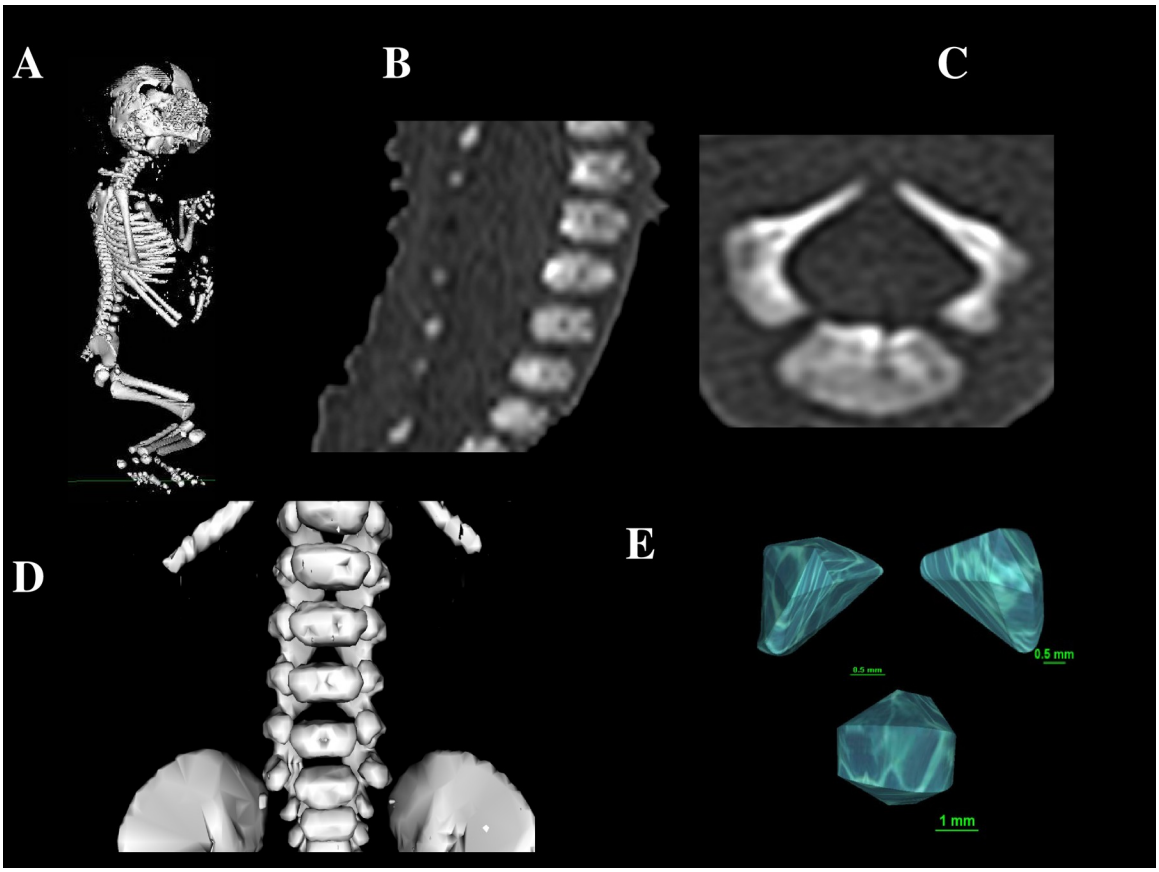

Figure 1. 3D reconstruction of CT of a female fetus aged 23 weeks in the sagittal (**A**) and transverse (**B**) projections of the lumbar vertebrae, reconstruction of the lumbar vertebrae in the frontal projection (**C**) with reconstruction of the ossification centers of L4 vertebrae using Osirix 3.9, and ossification centers of L4 vertebrae (**D**).

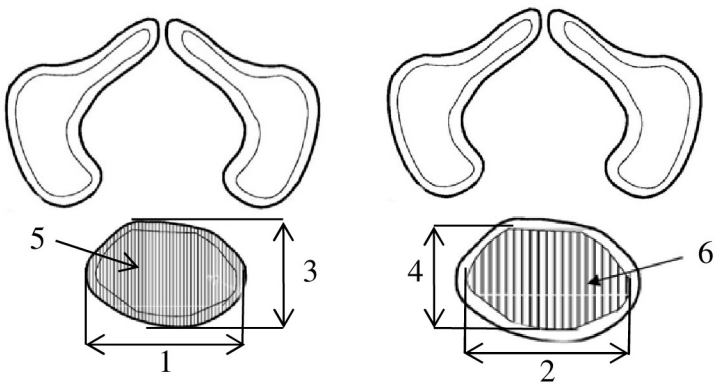

Figure 2. Diagram showing measurements of the body and ossification center of L4 vertebrae.

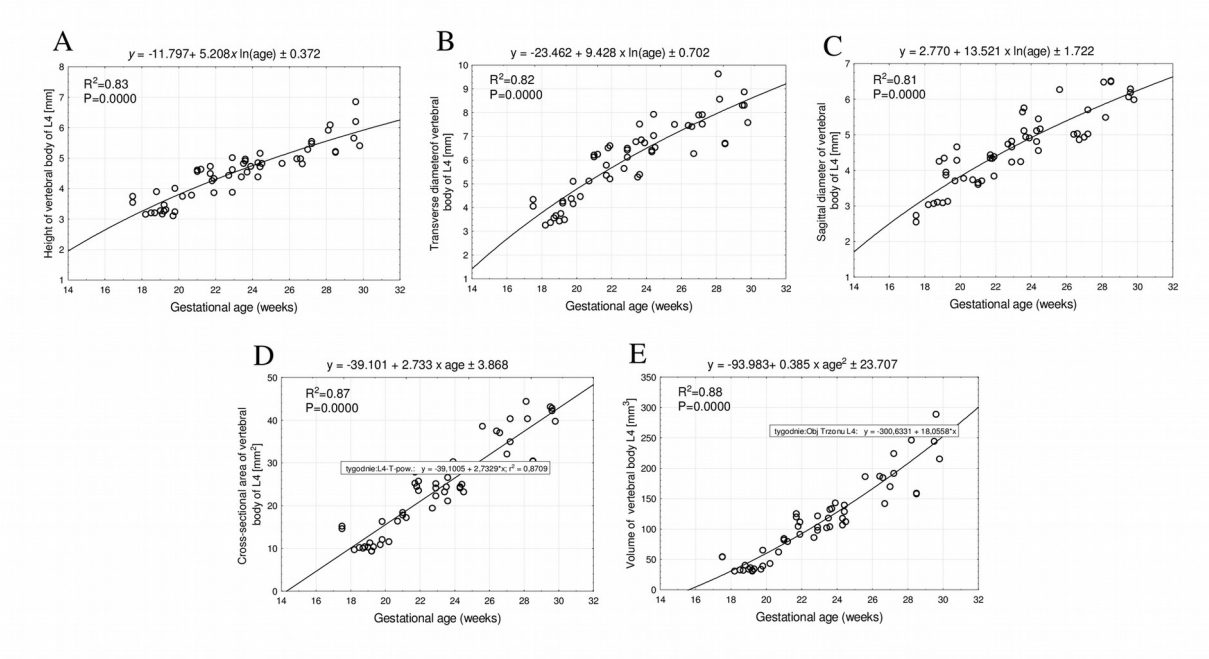

Figure 3. Regression lines for height (**A**) transverse diameter (**B**), sagittal diamteter (**C**) cross-sectional area (**D**) and volume (**E**) of vertebral body of L4.

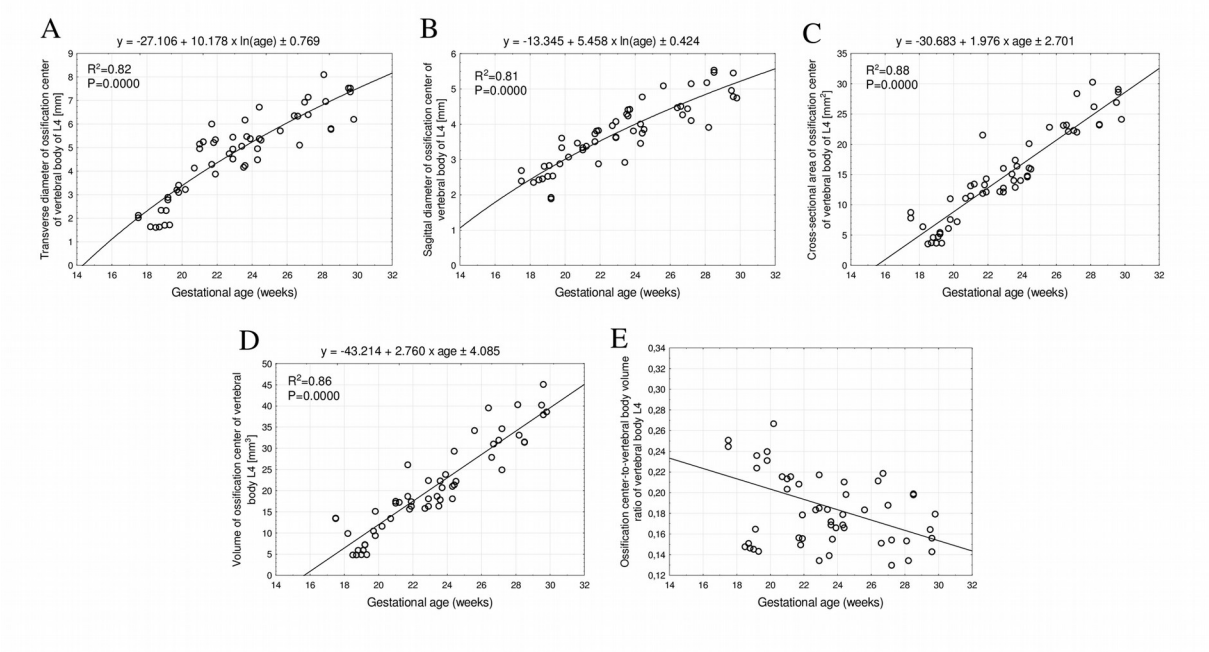

Figure 4. Regression lines for transverse diameter (**A**), sagittal diameter (**B**), cross-sectional area (**C**), and volume (**D**) of the ossification center of the L4 vertebral body and ossification center to vertebral body volume ratio of vertebral body of L4 (**E**).